

1 **Title: Quantification of alterations in diffusion measures of**
2 **white matter integrity associated with healthy aging**

3

4 Ciara J. Molloy^{1,2*,#a}, Sinead Nugent^{1,2}, Arun L.W. Bokde^{1,2}

5

6 ¹Cognitive Systems Group, Discipline of Psychiatry, School of Medicine, Trinity College Dublin,
7 Dublin, Ireland

8 ² Trinity College Institute of Neuroscience, Trinity College Dublin, Dublin, Ireland

9 ^{#a} Trinity Centre for Health Sciences, St. James's Hospital, Dublin, Ireland

10

11

12

13 *Corresponding author:

14 Email: molloycj@tcd.ie

15

16

17 **Abstract**

18

19 This study aimed to evaluate the linear association of age with diffusion tensor imaging (DTI)
20 measures of white matter such as fractional anisotropy (FA), mean diffusivity (MD), axial
21 diffusivity (AD) and radial diffusivity (RD). We assessed patterns of overlap between linear
22 correlations of age with FA with RD, MD and AD to characterize the process of white matter
23 degeneration observed with ageing. 79 healthy adults aged between 18 and 75 took part in the
24 study. The DTI data were based on 61 directions acquired with a b-value of 2000. There was a
25 statistically significant negative linear correlation of age with FA and AD and a positive linear
26 correlation with RD and MD, and AD. The forceps minor tract showed largest percentage of voxels
27 with an association of age with FA, RD and AD, and the anterior thalamic radiation with MD. We
28 found 5 main patterns of overlap: FA alone (15.95%); FA and RD (31.90%); FA and AD (12.99%);
29 FA, RD and AD (27.37%); FA RD, and MD (6.94%). Patterns of overlap between diffusion measures
30 may reflect underlying biological changes with healthy ageing such as loss of myelination, axonal
31 damage, as well as mild microstructural and chronic white matter impairments. This study may
32 provide information about causes of degeneration in specific regions of the brain, and how this
33 may affect healthy brain functioning in older adults.

34 **Introduction**

35

36 Diffusion tensor imaging (DTI) is a neuroimaging technique, which allows for non-invasive,
37 *in vivo*, investigation of white matter [1-3]. DTI measures are based on random motion of water
38 molecules, where within the brain diffusion of water is less restricted, or more isotropic, in areas
39 of grey matter and CSF, and more restricted, or more anisotropic, in areas of white matter. When
40 white matter structural architecture deteriorates, water molecules within white matter tissue
41 become more isotropic, making DTI a useful tool for assessing atrophy [4-9].

42

43 The diffusion tensor is a 3x3 covariance matrix used to model diffusion within a voxel, in
44 which there are 3 positive eigenvalues ($\lambda_1, \lambda_2, \lambda_3$) and 3 orthogonal eigenvectors ($\epsilon_1, \epsilon_2, \epsilon_3$). The
45 eigenvalues of the tensor give the diffusivity in the direction of each eigenvector. Together they
46 describe diffusion probability using an ellipsoid, where the axes of the ellipsoid are aligned with
47 the eigenvectors, and the major eigenvector (λ_1) represents the principal diffusion direction.

48

49 Fractional anisotropy (FA), mean diffusivity (MD), radial diffusivity (RD) and axial
50 diffusivity (AD) are the four main diffusion-based measurements of white matter structural
51 architecture. FA measures the amount of diffusion asymmetry within a voxel, where a value of 0
52 is isotropic and is represented by a spherical ellipsoid with equal eigenvalues, and a value of 1 is
53 anisotropic and is represented by an elongated ellipsoid with unequal eigenvalues. FA has been
54 associated with the microstructural integrity of white matter [10, 11]. RD is a measure of
55 perpendicular diffusivity and is an average of the two smaller eigenvalues ($\lambda_2+\lambda_3/2$). RD is

56 thought to reflect myelination of white matter tracts, where an increase in RD would suggest loss
57 of myelination [12-14], however white matter properties such as axonal diameter and density
58 changes also affect RD [10]. AD represents parallel diffusivity and is a measure of the largest
59 eigenvalue ($\lambda 1$). AD has been linked to axonal integrity, where a decrease in AD would suggest
60 axonal damage [15, 16]. AD decreases observed with axonal damage are thought to be caused
61 by increases in debris from disrupted membrane barriers [17], whereas increases in AD have been
62 suggested to reflect brain maturation [18]. However, increases in AD have also been linked to
63 severe white matter injury when observed with changes in FA and RD [19, 20]. MD, also known
64 as the apparent diffusion coefficient, is an average of all 3 eigenvalues in the tensor ($\lambda 1+\lambda 2+\lambda 3/3$),
65 and is therefore not independent of FA, RD and AD measures [10, 21]. It is thought to be a
66 measure of membrane density. Together all four of these diffusion measures can distinguish
67 distinct information about white matter microstructure.

68

69 The aging process coincides with changes in brain structure, brain function, and aspects
70 of cognition such that they all decline as we get older. Many DTI studies have examined white
71 matter structural changes that occur with aging [22-25]. Importantly, DTI studies of aging are
72 consistent with post mortem findings of axonal and myelin damage observed in older adults,
73 proving DTI to be a valuable *in vivo* measurement of white matter structural integrity [26, 27]. FA
74 is the most commonly studied diffusion measure, and extensive decreases in FA with normal
75 healthy aging have been reported in white matter across the brain including the body and genu
76 of the corpus callosum (CC), the uncinate fasciculus (UF), the internal and external capsule,
77 cingulum, fornix, the superior longitudinal fasciculus (SLF) and the inferior longitudinal fasciculus

78 (ILF) suggesting widespread alterations in white matter occur with aging [20, 28-32]. Along with
79 FA, age-related increases in MD have been reported in the genu and splenium of the CC [28], as
80 well as the fornix, UF [31], IFOF, SLF, and ILF [32]. RD increases have been reported in the
81 cingulum, CC, UF and ILF in older adults compared to younger adults [20, 21, 23, 33, 34]. Age-
82 related changes in AD are less consistent, with findings of decreases in AD in the fornix, internal
83 capsule, midbrain and cerebellum, but also reports of increases in AD in the CC [20, 23, 33].
84 However, other studies have also reported no changes in AD in older adults compared to younger
85 adults [34-36], suggesting that perhaps AD changes are more subtle than RD. Further, studies
86 showing greater RD changes compared to AD with aging indicate that myelination loss may be
87 the main cause of degeneration of white matter with healthy aging [20, 25, 33, 34]. Longitudinal
88 studies of older adults have shown global FA and MD changes, as well as FA, RD and AD changes
89 in the genu of the CC within two years, suggesting that alterations in white matter can indeed
90 occur over short periods of time with increased age [23, 37]. It has also been shown that white
91 matter continues to mature in adulthood, with FA continuing to increase and MD continuing to
92 decrease until between the ages of 20-42 years and 18-41 years respectively [38], stressing the
93 importance of considering age-related changes across adulthood. Importantly maturation of
94 white matter occurs at different rates across the brain, suggesting that perhaps the rate
95 degeneration occurs differently in different tracts [23, 38].

96

97 Patterns of white matter changes within the brain have been examined to better
98 understand and define the aging process, however conflicting findings have been reported. One
99 pattern is the anterior-posterior gradient of degeneration, in which greater differences in FA in

100 frontal regions compared to posterior regions of the brain; however although studies have
101 reported this pattern, others have found no evidence of this [23, 33, 39]. Further, studies have
102 even reported the opposite gradient pattern of larger FA decreases in posterior regions
103 compared to frontal regions [33, 40]. A second proposed pattern is the superior–inferior gradient
104 of white matter degeneration which postulates that superior white matter is more vulnerable to
105 age-related changes [31, 41]. A study by Sullivan and colleagues (2010) reported both the
106 anterior-posterior gradient and superior-inferior gradient of age-related changes in the brain
107 indicating that perhaps age-related white matter changes may be more complex than one
108 gradient of degeneration. A third pattern, described as the myelodegeneration hypothesis,
109 proposes that myelin degeneration during aging occurs in the opposite direction of development
110 [12-14]. This pattern would therefore be consistent with age-related changes in RD in white
111 matter fibers that are last to myelinate, such as frontal and temporal associations fibers. Davis
112 and colleagues (2009) reported age-related RD changes in the CC, cingulum and UF, along with
113 larger age-related RD changes compared to AD, supporting the myelodegeneration hypothesis
114 (Davis et al. 2009). However, again another study found no evidence of this pattern of age-related
115 degeneration [42]. The inconsistent findings across the literature further suggest that these
116 interpretations of white matter changes may be a simplification of the aging process, highlighting
117 the need for a more thorough understanding of age-related effects on white matter.

118

119 While studies assessing age-related changes in diffusion measures separately have been
120 informative, a combined analyses of FA, MD, RD and AD may provide a more comprehensive
121 understanding of the underlying biological profile of the breakdown of white matter observed

122 with aging [11, 24]. Indeed, a few studies quantifying specific patterns of changes in diffusion
123 measures of white matter have proposed a more complex and region-specific interpretation of
124 disruption observed with aging [20, 33]. Burzynska and colleagues (2010) quantified the
125 frequency of overlap in age-related differences in measures of FA, RD and AD along with MD. A
126 comparison of young and older adults established five main patterns of differences in diffusion
127 measures observed with aging: (1) decreased FA with increased RD thought to reflect
128 demyelination; (2) decreased FA with increased RD and MD thought to reflect chronic stages of
129 white matter fiber degeneration; (3) decreased FA only thought to reflect mild microstructural
130 alterations; (4) decreased FA with decreased AD thought to reflect acute axonal damage; and (5)
131 decreased FA and AD with increased RD thought to reflect secondary Wallerian degeneration
132 resulting in axonal loss and increased extracellular matrix tissue structures (Burzynska et al.
133 2010). Another study comparing younger and older adults assessed the overlap between FA, RD
134 and AD measures and found three main patterns of age-related changes in diffusion measures;
135 (1) decreased FA with increased RD only; (2) decreased FA and AD with increased RD; and (3)
136 decreased FA, with both increased AD and RD (Bennett et al. 2010). Another study by Zhang and
137 colleagues (2010) of young, middle-aged and older adults also looked at the concordance and
138 discordance of FA age-related changes with MD, and RD with AD separately [43]. Unlike the two
139 previous studies mentioned, this study did not focus the analysis on voxels with showing
140 significant age-related FA changes. They found (1) regions of decreased FA with increased MD
141 increases and related it to demyelination and axonal loss, (2) regions of MD increases with no FA
142 decreases and interpreted it as inconclusive, (3) one region with FA decreases and no MD changes
143 and related it to Wallerian degeneration, (4) a greater change in RD than AD and suggested it

144 reflected demyelination and Wallerian degeneration, and finally (5) a one region with greater
145 increase in AD than RD and reported this as inconclusive. These studies emphasize the
146 importance of considering patterns of changes in diffusion measures to elucidate and define the
147 specific profiles of age-related alterations in white matter regions across the brain.

148

149 The first goal of this study was to examine patterns of overlap between linear correlations
150 of age with FA, RD, AD and MD in a cohort of young, middle-aged and older adults. Specifically,
151 we quantified the frequency of patterns to establish the most prominent to least prominent
152 pattern. Many previous studies assessing patterns of overlap between multiple diffusion
153 measures have compared young and old adults [20, 33]. These studies have typically employed
154 voxelwise statistical analyses of DTI data with a b-value of 1000; in the current study we used a
155 higher b-value of 2000. We hypothesized that specific patterns of overlap between linear
156 correlations of age with FA, RD, AD and MD would be observed, and that these different patterns
157 may reflect specific regions of minor microstructural alterations, axonal damage, loss of
158 myelination, and regions of more chronic white matter degeneration which are all thought to
159 occur in aging. Examination of the patterns of overlap between linear changes in diffusion
160 measures with age will complement previous studies examining differences between young and
161 old.

162

163

164 **Materials and methods**

165

166 **Participants**

167

168 Seventy-nine, right-handed participants aged between 18 and 75 years (mean = 43.9 ±
169 18.33 SD) (male = 39) took part in the study. Exclusion criteria included permanent metallic
170 objects in the body, a self-reported history of psychiatric or neurologic disorders or a history of a
171 serious head injury. For participants over the age of 55 the Mini Mental State Exam (MMSE) was
172 performed and participants with scores below 1.5 SD of the standardized scores were excluded
173 from the study (Table 1).

174

175 **Table 1. Participant demographics.**

	Overall (n=79)	Young (n=33)	Middle (n=16)	Older (n=30)
Age	43.91(18.33)	24.66 (5.32)	46.25 (5.81)	63.83 (4.46)
Gender (M:F)	39:39	18:15	7:9	14:16
NART	33.04 (5.66)	32.97(5.75)	31.44 (5.29)	35.40 (6.03)
	113.59		111.94	
NART IQ	(4.78)	112.63 (3.92)	(4.84)	115.53 (5.09)
MMSE	-	-	-	29.33 (0.76)
WMH load (%)	0.06 (0.10)	0.04 (0.08)	0.09 (0.15)	0.06 (0.08)

176 Measures are displayed as mean (±SD).

177

178 This study was approved by the Faculty of Health Sciences review board at Trinity College
179 Dublin. Written, informed consent was obtained from all participants in accordance with the
180 tenants of the Declaration of Helsinki. Participants were recruited through advertisements in
181 local newspapers, church newsletters, and poster campaigns throughout universities in Dublin.

182

183 **MRI data acquisition**

184

185 Whole-brain high angular resolution diffusion imaging (HARDI) data were acquired on a Philips
186 Intera Achieva 3T MRI system (Best, The Netherlands) equipped with a 32-channel head coil at
187 Trinity College of Institute of Neuroscience, Dublin. DWI data were collected using a single-shot
188 echo-planar imaging sequence with echo time = 81 ms, repetition time = 14,556 ms, FOV 224mm,
189 matrix 112x112, isotropic voxel of 2x2x2 mm, 65 slices of 2 mm thickness with no gap between
190 slices. Diffusion gradients were applied in 61 directions, with $b = 2000 \text{ s/mm}^2$, and four $b = 0$
191 s/mm^2 were acquired also. A 3D high resolution T1-weighted anatomical image was collected
192 using a T1FFE (fast field echo) sequence with echo time = 3.8 ms, repetition time = 8.4 ms, FOV
193 230mm, 0.9x0.9x0.9 mm voxel size, 180 slices, for correction of EPI-induced geometrical
194 distortions in the data. A T2-weighted fluid-attenuated inversion recovery (FLAIR) image was
195 collected with echo time = 120 ms, repetition time = 11000 ms, 0.45x0.45 mm² in-plane
196 resolution, slice thickness = 5 mm, FOV = 230 mm.

197

198 **Estimated total intracranial volume**

199

200 FreeSurfer image analysis suite version 5.3 (<http://surfer.nmr.mgh.harvard.edu/>) was
201 used to perform automated volumetric segmentation of the T1-weighted anatomical image and
202 extract estimated total intracranial volume (eTIV) for white matter hyperintensity load analysis
203 [44].

204

205 **White matter hyperintensity volume**

206

207 Automated segmentation of white matter hyperintensity (WMH) volume (ml) was
208 calculated using the lesion segmentation toolbox (LST) version 2.0.15 (www.statistical-
209 modelling.de/lst.html) for SPM12. T2-weighted FLAIR images were used for lesion segmentation,
210 with T1-weighted anatomical images as a reference. Lesions were segmented using the lesion
211 prediction algorithm, which consists of a binary classifier in the form of a logistic regression model
212 trained on the data of 53 multiple sclerosis patients with severe lesion patterns obtained at the
213 Department of Neurology, Technische Universität München, Munich, Germany. As covariates for
214 this model a similar lesion belief map as for the lesion growth algorithm [45] this was used, as
215 well as a spatial covariate that takes into account voxel specific changes in lesion probability.
216 Parameters of this model fit are used to segment lesions in new images by providing an estimate
217 for the lesion probability for each voxel. To describe WMH load quantitatively WMH volume was
218 normalized by eTIV extracted from FreeSurfer analysis.

219

220 **Preprocessing of DWI data**

221

222 DWI data were preprocessed using ExploreDTI (v4.8.4) software (www.exploredti.com/)
223 (Leemans et al. 2009a). Data quality checks were performed, including visual inspection of correct
224 orientation of gradient components and checking for gross artifacts. The data were corrected for
225 motion correction, eddy current induced geometric distortions and for echo-planar imaging (EPI)
226 deformations by co-registering and resampling to each subjects' T1-weighted anatomical image
227 [46]. Correction for each of these distortions was performed in one step. The B-matrix rotation
228 was performed within this step to reorient the data appropriately [47]. The default setting of
229 robust extraction of kurtosis indices with linear estimation (REKINDLE) approach was utilized
230 when the tensor model was applied to the data [48].

231

232 **TBSS analysis**

233

234 FSL software (FMRIB Software Library- <http://www.fmrib.ox.ac.uk/fsl/>) [49] was
235 employed to perform whole brain voxel-wise analysis of white matter using Tract Based Spatial
236 Statistics (TBSS) [50]. FA diffusion images were extracted from diffusion data preprocessed using
237 ExploreDTI.

238

239 A study specific template was created using all 79 subjects by aligning each subject's FA
240 image to every other subject's FA image to identify the most representative subject. The study

241 specific template chosen was then affine aligned to MNI standard space (included in FSL software
242 package). Every other subject's FA image was then warped into MNI space by combining the non-
243 linear transformation to the chosen template FA image with the affine transformation to MNI
244 space. This is done in one step to avoid resampling of the images twice. FA images from all
245 subjects were then averaged to create the mean FA template and thinned to create a mean FA
246 skeleton which represented the 'skeletons' of all tracts common to the group. We also
247 investigated other diffusion measures extracted from data preprocessed in ExploreDTI such as
248 MD, RD and AD. To do this we applied the same non-linear transformation and skeleton
249 projection used for the FA images to the MD, RD and AD diffusion measures.

250

251 **Statistical Analysis**

252

253 Voxel-wise statistics were performed using the randomise permutation-based inference
254 tool for nonparametric statistical thresholding within FSL [51]. Permutation methods were
255 employed as they are employed when the null distribution is not known. A linear correlation of
256 age with each diffusion measure was performed, with WMH load, the National Adult Reading
257 Test (NART) and gender included as covariates of no interest. The NART provides an estimate
258 measure of premorbid intelligence [52]. As intelligence and gender differences in diffusion
259 measures of white matter have been reported, we controlled for the effects of these measures
260 in our analysis [32, 53]. It has also been suggested that WMH should be adjusted for when
261 examining differences in healthy white matter [54]. In our supplementary material we provide
262 the same analysis without any covariates included to compliment previous studies (see

263 supplementary Table 1). The mean FA skeleton for the group was used as mask (thresholded to
264 a value of 0.2) and the number of iterations was set to 10,000. The results were thresholded to a
265 p value of <0.05 corrected for multiple comparisons across voxels using the threshold-free cluster
266 enhancement (TFCE) option from the randomize permutation testing tool in FSL [55].

267

268 **Quantification of age-related white matter results**

269

270 To quantify the size of the clusters of significant age-related linear correlations with
271 diffusion measures across the whole brain, the percentage of voxels associated with aging was
272 calculated by dividing the number of voxels showing statistically significant linear correlations
273 with age for FA, MD RD and AD by the total number of voxels in the mean FA skeleton.

274

275 To quantify the age-related linear correlations with diffusion measures within white
276 matter tracts ROIs were created using the JHU Tractography atlas. Specifically, each ROI was
277 masked, thresholded to above 10, and multiplied by the mean_FA_skeleton to create masks of
278 total voxels within each tract. Statistically significant results for each diffusion measure were
279 multiplied by tract ROIs to create masks of voxels showing linear correlations with age. The
280 percentage of age-related voxels within tract ROIs was calculated by dividing FA, RD, AD and MD
281 masks of linear correlations with age by the total tract masks.

282

283 **Quantification of overlap between diffusion measures**

284

285 The overlap between voxels showing age-related linear correlations with FA, MD, RD and
286 AD was assessed. First the TBSS results showing significant linear correlations of age with FA, MD,
287 RD and AD were masked. Then the FA mask was multiplied by each of the MD, RD and AD masks
288 to create masks of the overlap between diffusion measures. The percentage of overlapping
289 voxels was calculated by dividing each of the overlap masks by the FA mask.

290

291 **Results**

292

293 All statistically significant linear correlations of diffusion measures with age reported in
294 the results include WMH load, NART scores and gender as covariates to account for any changes
295 in diffusion measures of white matter that may be related to them.

296

297 **Age-related linear correlations with diffusion measures**

298

299 We quantified the age-related linear correlations in each of the diffusion metrics by
300 calculating the percentage of voxels showing statistically significant linear correlations with age,
301 with NART and gender included as covariates (Table 2). Age-related statistically significant
302 negative linear correlations with FA were observed in 49.69% of white matter voxels, statistically
303 significant positive linear correlations with RD were observed in 40.00%, statistically significant
304 positive linear correlations with MD in 7.73%, statistically significant negative linear correlations

305 with MD were observed in 0.41%, statistically significant positive linear correlations with AD in
306 0.31%, and statistically significant negative linear correlations with AD in 31.53% of white matter
307 voxels. There were no statistically significant positive linear correlations of FA with age or
308 statistically negative linear correlations of RD with age.

309

310 **Table 2. Total number and percentage of voxels correlated with age, and the overlap of MD,**
311 **RD and AD with age-related FA voxels.**

	FA	FA↓	MD↑	MD↓	RD↑	AD ↑	AD ↓
skeleton							
Total no. of voxels with age-related correlations	128259	63740	9909	529	50015	398	40528
Total % of voxels with age-related correlations*	-	49.69%	7.73%	0.41%	40.00%	0.31%	31.53%
No. of voxels overlapping with FA voxels	-	-	6680	477	44967	134	27502
% of voxels overlapping with FA voxels**	-	-	10.49%	0.75%	70.55%	0.21%	43.14%

312 WMH load, NART and gender were included as covariates.

313 * This is calculated as total number of FA/MD/AD/RD voxels correlated with age divided by total
314 no. of FA_skeleton_mask voxels.

315 **This is calculated as no. of overlapping voxels divided by total no. of FA voxels.

316

317 We then assessed percentage of white matter regions affected by aging using the JHU
318 white matter tractography atlas (Table 3). FA, RD and AD all showed the greatest percentage of
319 voxels correlated with age in the forceps minor (90.28%, 81.73% and 71.17% respectively),
320 whereas MD showed the greatest percentage of voxels correlated with age in the right anterior
321 thalamic radiation (16.22%). All tracts showed some percentage of voxels with age-related linear
322 correlations with FA and RD; however, the cingulum hippocampus showed the smallest
323 percentage (FA: 2.71% and 2.33% for left and right respectively; RD: 0.78% and 3.10% for left and
324 right respectively). For MD and AD, there were no voxels with age-related statistically significant
325 positive or negative linear correlations in the cingulum hippocampus.

326

327

328

329

330

331

332

333

334

335

336
337
338
339
340
341
342
343
344
345
346
347
348
349
350
351
352
353
354
355
Table 3. Number and percentage of voxels showing age-related correlations with diffusion measures.

Tract		Total	FA↓	RD↑	MD↑	MD↓	AD↑	AD↓	FA↓%	RD↑%	MD↑%	MD↓%	AD↑%	AD↓%
Anterior Thalamic Radiation	L	4463	2440	2271	502	0	11	2150	54.67	50.89	11.25	0.00	0.45	48.17
	R	4413	2774	2575	716	62	0	1875	62.86	58.35	16.22*	1.40	0.00	42.49
Cingulum	L	611	386	335	9	0	0	191	63.18	54.83	1.47	0.00	0.00	31.26
	R	220	62	47	4	0	0	8	28.18	21.36	1.82	0.00	0.00	3.64
Cingulum Hippocampus	L	258	7	2	0	0	0	0	2.71	0.78	0.00	0.00	0.00	0.00
	R	258	6	8	0	0	0	0	2.33	3.10	0.00	0.00	0.00	0.00
Corticospinal	L	2559	1559	1368	76	0	0	1629	60.92	53.46	2.97	0.00	0.00	63.66
	R	2539	1318	938	326	255	0	1458	51.91	36.94	12.84	10.04*	0.00	57.42
Forceps Major	B	3764	2319	1869	261	0	0	701	61.61	49.65	6.93	0.00	0.00	18.62
Forceps Minor	B	5698	5144	4657	794	0	64	4055	90.28*	81.73*	13.93	0.00	1.24*	71.17*
Inferior Fronto Occipital Fasiculus	L	4896	3439	2959	420	0	0	1549	70.24	60.44	8.58	0.00	0.00	31.64
	R	5628	4135	3744	710	0	0	2122	73.47	66.52	12.62	0.00	0.00	37.70
Inferior Longitudinal Fasiculus	L	3893	2194	1655	399	0	0	969	56.36	42.51	10.25	0.00	0.00	24.89
	R	3088	1930	1354	11	0	0	646	62.50	43.85	0.36	0.00	0.00	20.92
Superior Longitudinal Fasiculus	L	4631	2751	2239	29	0	0	195	59.40	48.35	0.63	0.00	0.00	4.21
	R	4878	2853	2488	444	0	0	494	58.49	51.00	9.10	0.00	0.00	10.13
Superior Longitudinal Fasiculus Temp	L	2185	1353	1059	27	0	0	63	61.92	48.47	1.24	0.00	0.00	2.88
	R	2240	1238	1030	209	0	0	147	55.27	45.98	9.33	0.00	0.00	6.56
Uncinate Fasiculus	L	2192	1346	1013	49	0	0	1191	61.41	46.21	2.24	0.00	0.00	54.33
	R	1183	661	434	141	0	0	642	55.87	36.69	11.92	0.00	0.00	54.27

WMH load, NART and gender were included as covariates. The JHU white matter tractography atlas was used to create tract ROIs.

*This indicates the white matter tract with the largest percentage of voxels linearly correlated with age.

356 **Overlap between age-related linear correlations with diffusion**

357 **measures**

358

359 Within FA voxels showing significant negative age-related linear correlations, we
360 calculated the percentage of voxels also showing statistically significant linear correlations of age
361 with each of the diffusion measures of MD, RD and AD (Fig 1 and Table 4). Voxels showing
362 statistically significant positive age-related linear correlations with RD overlapped with 70.55%
363 of voxels showing statistically significant negative age-related linear correlations with FA. Positive
364 and negative statistically significant linear correlations with AD overlapped with 0.21% and
365 43.14% of voxels showing statistically significant negative age-related linear correlation FA
366 respectfully. Positive and negative statistically significant linear correlations with MD overlapped
367 with 10.49% and 0.75% of voxels showing negative age-related statistically significant linear
368 correlations with FA respectfully.

369

370 **Table 4. Total number and percentage of voxels correlated with age showing specific patterns of**
371 **overlap between diffusion measures.**

	FA↓ alone	FA↓&RD↑ only	FA↓&AD ↓ only	FA↓,AD ↓&RD↑	FA↓,AD↓, RD↑&MD ↑	FA↓,RD ↑&MD ↑
No. of voxels	10164	20335	8283	17447	941	4421
overlapping with						

FA voxels						
% of voxels	15.95%	31.90%	12.99%	27.37%	1.48%	6.94%
overlapping with						
FA voxels*						

372 WMH load, NART and gender were included as covariates.

373 *This is calculated as no. of overlapping voxels divided by total no. of FA voxels (63740).

374

375 **Fig 1. Overlap between statistically significant linear correlations of age with FA and RD, AD**

376 **and MD.** Age-related positive correlations with RD overlapped with 69% of age-related negative

377 correlations with FA; AD positive correlations overlapped with 43% of FA correlations; and MD

378 with 8%. Images are displayed in radiological convention (i.e. left=right). FA = blue; RD, AD, MD

379 = red; Overlap = green.

380

381 We further identified 5 main patterns of overlap between diffusion measures in white

382 matter regions showing age-related negative linear correlations with FA, and a sixth pattern in

383 very few voxels (Fig 2 and Table 4):

384

385 **Fig 2. Patterns of overlap between diffusion measures within voxels showing age-related**

386 **correlations with FA.** Images are displayed in radiological convention (i.e. left=right). FA alone =

387 blue; FA & RD = pink; FA & AD = red; FA, RD&AD = green; FA, RD & MD = yellow; FA, RD, AD &

388 MD = light blue.

389

390 1. FA and RD only pattern: statistically significant positive age-related linear correlations
391 with RD alone showed the greatest percentage of overlapping voxels with FA across the brain
392 (31.90%). This was the main pattern observed in the forceps major, right and left SLF, right and
393 left ILF, right and left IFOF and right cingulum. This pattern was also observed in the right and left
394 anterior thalamic radiation, and smaller clusters of the right and left UF, corticospinal tract, and
395 forceps minor and body of the CC, and right anterior limb of the internal capsule.

396

397 2. FA, RD and AD pattern: statistically significant negative age-related linear correlations
398 with AD and statistically significant positive age-related linear correlations with RD showed the
399 second greatest percentage of overlapping voxels with FA linear correlations (27.37%). This was
400 the main pattern observed in the forceps minor, right and left UF, right and left corticospinal
401 tract, left posterior limb of the internal capsule, and left cres of the fornix. This pattern was also
402 observed in a large number of voxels in the left and right IFOF, the left retrolenticular part of the
403 internal capsule, and smaller number of voxels in the right and left ILF, SLF, and the forceps major.

404

405 3. FA only pattern: statistically significant negative age-related linear correlations with FA
406 alone showed the third greatest percentage of overlapping voxels (15.95%). This was not the
407 main pattern in any tract ROI. It was observed in the right and left SLF and temporal SLF, as well
408 as small regions of the right and left anterior thalamic radiation, cingulum, forceps major and
409 minor (body and left splenium of the CC), right and left IFOF, ILF and UF, right internal capsule
410 and the left external capsule.

411

412 4. FA and AD pattern: The fourth pattern observed was age-related statistically significant
413 negative linear correlations with AD and FA (12.99%). This was the main pattern observed in the
414 right UF along with the FA, AD and RD pattern. It was also observed in clusters of the forceps
415 major and minor, right and left anterior thalamic radiation, right and left corticospinal tract, right
416 and left IFOF, right and left ILF as well as the right SLF and left UF, small clusters of the of the right
417 external capsule, and the retrolenticular part of the right internal capsule, as well as right and left
418 internal capsule.

419

420 5. FA, RD and MD pattern: The fifth pattern observed was age-related statistically significant
421 positive linear correlations with RD and MD, with statistically significant negative linear
422 correlations with FA (6.94%). This pattern was the main pattern in the fornix (column and body).
423 It was also found in small regions of the forceps minor (also genu and body of the CC), and the
424 right and left anterior thalamic radiation, right anterior IFOF and posterior IFOF/ILF, right
425 corticospinal tract, forceps major, right and left SLF, and right and left anterior thalamic radiation.

426

427 6. FA, RD, AD, and MD pattern: The sixth pattern observed was age-related statistically
428 significant negative linear correlation with FA and AD, with statistically significant positive linear
429 correlations with MD and RD 1.48%). This pattern was found in a small cluster of voxels in the
430 right IFOF, right and left UF, the forceps minor and body of CC, and right SLF.

431

432 **Discussion**

433

434 **General findings**

435

436 This study aimed to quantify the linear effect of age on FA, RD, AD and MD diffusion
437 measures of white matter integrity in a cohort of young, middle aged and older healthy adults,
438 after adjusting for white matter hyperintensity (WMH) load, premorbid IQ (NART) and gender.
439 Our findings showed negative linear correlations of age with FA and AD, as well as MD in a small
440 number of voxels. We also found a positive linear correlation of age with MD and RD, as well as
441 AD in a small number of voxels.

442

443 The findings of negative correlations of FA with healthy aging in many regions of the brain
444 is in accordance with decreased FA in older adults compared to younger adults in many previous
445 studies [21, 23-25, 29, 33, 39, 56]. When we quantified the number of voxels linearly correlated
446 with age our findings showed that FA was statistically significant correlated with age in
447 approximately half of the brain's white matter, higher than all other diffusion measures. This was
448 similar to the findings from a study by Burzynska and colleagues (2010) showing age-related
449 decreases in FA in 53% of voxels. We further showed that the tract with the highest percentage
450 of voxels showing age-related linear correlations with FA was the forceps minor, which was also
451 true for RD and AD, suggesting that this tract may be greatly affected by typical aging.
452 Interestingly age-related associations with FA were found in approximately 50% of voxels or more
453 in all tracts except the right cingulum, and the right and left cingulum hippocampus, which is

454 consistent with the parahippocampal segment of the cingulum. This points to generally extensive
455 global effects of healthy aging on white matter integrity. The small number of voxels showing
456 associations of age with FA and RD in the hippocampal branch of the cingulum, and the lack of
457 any association with AD or MD indicates this region of white matter is less affected than other
458 white matter tracts. Similar to our findings, a study comparing young and older healthy adults
459 found differences in the subgenual branch of the cingulum but no change in any diffusion
460 measures in the parahippocampal segment of the cingulum [57].

461

462 Our analysis revealed a larger percentage of voxels showing linear correlations of age with
463 RD (positive = 40.00%; negative = 0%) than with AD (positive = 0.31%; negative = 31.53%) and
464 MD (positive = 7.73%; negative = 0.41%) indicating more widespread changes in RD across the
465 brain with aging. In line with our initial findings, greater changes in RD compared to AD with aging
466 has been reported previously suggesting that healthy aging is more affected by myelination loss
467 than axonal damage across the brain [20, 33, 34, 43].

468

469 Unlike Burzynska and colleagues (2010) we found only a small number of voxels with
470 negative linear correlations of age with MD. However, this is a less consistent finding in the
471 literature, with more studies reporting an increase in MD with aging [21, 28, 31, 32]. We also
472 found a small number of voxels showing a positive linear correlation of age with AD. Both
473 increases and decreases of AD with age have been reported [20, 23, 33, 57]. Animal studies have
474 attributed decreases in AD to acute axonal injury [13, 58]. Human diffusion studies have observed
475 AD increases with traumatic brain injury, resulting in more chronic and irreversible white matter

476 damage [59]. Taking this into account, perhaps the cohort in the current study had less chronic
477 axonal damage than previous studies. However, another explanation for AD increases may be
478 due to loss of fiber coherence in regions of crossing fibers, which is a common issue with the
479 diffusion tensor model [60].

480

481 To further inform age-related changes in white matter integrity we next assessed patterns
482 of overlap between diffusion measures significantly linearly correlated with age. Specifically, we
483 examined patterns only within voxels showing significant negative linear correlations of age with
484 FA. That RD overlapped with ~70% and AD with ~43% of voxels showing age-related linear
485 correlations with FA, is indicative of a strong association of both RD and AD with aging in our
486 cohort. The greater percentage of overlap between FA and RD than FA and AD, further suggests
487 that loss of myelination may be a major contributor to degeneration observed with healthy aging
488 [33, 34].

489

490 While our results showed multiple patterns of overlapping diffusion measures within
491 tracts, a main pattern was observed for most tracts. Multiple patterns of overlap within tracts
492 may reflect vulnerability in specific regions of the brain, rather than white matter tracts as a
493 whole. It is also possible that examination of patterns of overlap reveals regions of white matter
494 tracts showing different stages of white matter changes observed with aging, or simply that
495 perhaps degeneration is not consistent across the brain, which would not be surprising given that
496 some studies have suggested different gradients of changes in diffusion of white matter integrity
497 with aging [31, 34, 61]. However, given that a main pattern was observed in many tracts including

498 the forceps minor, forceps major, left and right SLF and ILF, our findings suggest there may be a
499 specific profile of age-related changes in major white matter fiber bundles.

500

501 **The FA and RD pattern**

502

503 The most prominent pattern observed was a linear correlation of age with FA and RD, but not
504 AD, which has been thought to reflect mainly the process of myelination loss in white matter
505 tracts [13, 14, 20, 33]. Histology investigations have indicated that white matter atrophy is a
506 major causal factor of brain degeneration with aging, supporting DTI studies [27]. Further, loss of
507 myelination in the CC, a highly myelinated white matter bundle, for which the genu and splenium
508 sub regions are consistent with the forceps major and minor respectively, has been shown in
509 older adults [27]. Consistent with this, in the current study the FA and RD pattern was largely
510 observed in the forceps major, along with the IFOF, ILF and SLF. Similarly, Burzynska and
511 colleagues' (2010) study comparing older and younger adults also reported this pattern as the
512 dominant pattern in forceps major [20].

513

514 Differences in white matter integrity in the SLF with aging have been reported previously
515 [62], as well as the FA and RD pattern of age-related changes in the SLF [33]. Although the FA and
516 RD pattern was the prominent pattern in the SLF, it should be noted that we also found voxels
517 showing the FA alone pattern in both the left and right SLF as well as the FA, AD and RD pattern
518 and FA, RD and MD pattern in a small number of voxels of the right SLF.

519

520 For the ILF and IFOF findings, it is important to note that they are known to overlap partly,
521 so diffusion measures may not distinguish between these tracts very well along some regions
522 [63]. We also found some clusters of voxels within both tract ROIs showing other patterns.
523 Previous studies of age-related changes in the IFOF are mixed. One previous study examining
524 frontal lobe white matter connections, did not find age-related linear correlations with diffusion
525 measures in this tract [62]. However, differences in FA have been reported in older adults
526 compared to young [31, 32, 64]. It is possible that these discrepancies across studies may reflect
527 differences in DTI acquisition parameters or analysis techniques. Overall, it seems that loss of
528 myelination may indeed explain a large proportion of white matter degeneration observed with
529 aging.

530

531 **The FA, RD and AD pattern**

532

533 The FA, RD and AD pattern has been linked to axonal damage, gliosis and subsequent
534 increases in extracellular tissue structures [3, 20]. While decreases in AD have been reported in
535 studies of ischemic stroke, which have been suggested to result in gliosis. This was the main
536 pattern in many tracts with frontal lobe connections such as the forceps minor, anterior thalamic
537 radiation, UF, and a large proportion of the IFOF, as well as other white matter fibers such as the
538 corticospinal tract and the cres of the fornix, and cingulum.

539

540 The frontal lobes have been suggested to be sensitive to aging [20, 33, 41]. Although
541 studies have indicated that frontal regions may be more vulnerable to age-related decline than

542 posterior regions [41], a longitudinal study assessing rate of change in diffusion measures did not
543 find evidence of the anterior-posterior gradient over a 2-year period [23]. Our findings of
544 widespread age-related degeneration in white matter, with multiple patterns across the brain
545 also indicate that the pattern of degeneration may be more complicated. For example, although
546 the FA, RD and AD pattern was the main pattern in the UF, some voxels showed the FA and RD
547 pattern, as well as the FA and AD pattern. Interestingly, a previous study assessed diffusion
548 measures separately and found changes in FA, RD, AD and MD with aging in the UF, suggesting
549 that an overlap in age-related changes could have also been observed in the UF [31].

550

551 The cingulum, which connects the frontal lobe with parietal and temporal regions such as
552 the hippocampus and parahippocampus, showed the FA, RD and AD pattern in the right and left
553 cingulum, as well as a similar number of voxels with the FA and RD pattern in the left cingulum
554 [65-67]. However, only a very small number of voxels within the cingulum hippocampus ROI were
555 associated with aging suggesting that this tract was not affected by age. Other studies have also
556 observed differences in FA and RD only in parts of the cingulum, such as the superior portion but
557 not posterior or inferior region [31], and the subgenual branch but not the parahippocampal
558 segment of the cingulum [57].

559

560 This FA, RD and AD pattern was also reported in the crus of the fornix by a previous study
561 comparing younger and older adults, suggesting this small white matter structure is vulnerable
562 to healthy aging possibly due to axonal damage and gliosis [20]. Our findings suggest that axonal

563 damage and increases in extracellular matrix tissues may be another major cause of brain white
564 matter changes that occur with the normal healthy aging process.

565

566 **The FA alone pattern**

567

568 The FA alone pattern has been suggested to reflect mild microstructural changes, such as
569 fiber structure loss without any major tissue loss, where these decreases in FA in the absence of
570 MD increases may be due to subtle changes in RD and AD [20, 43]. Although this pattern was
571 observed throughout the brain, it was not the most prominent pattern in any white matter tract.
572 This indicates that FA overlapped with other diffusion measures in a large proportion of voxels
573 showing age-related linear correlations. Consistent with the straight gyrus reported by Burzynska
574 and colleagues (2010), we also observed the FA alone pattern in the inferior frontal gyrus. Overall
575 the current study findings suggest that these less severe microstructural changes occur across
576 the brain with aging. The fact that FA showed the largest percentage of affected voxels, indicates
577 that perhaps FA alone mild may changes occur first, may then be followed by changes and/or
578 greater changes in other diffusion measures. Future studies comparing young and middle aged
579 adults or longitudinal designs are needed to investigate this further.

580

581 **The FA and AD pattern**

582

583 The FA and AD pattern was the fourth pattern we observed which has been linked to
584 acute axonal damage, such as axon swelling and fragmentation, and therefore distinguishing it
585 from the FA, RD and AD pattern [20]. Although this pattern was observed in a proportion of voxels
586 in many tract ROIs, it was not the dominant pattern in any tract. This indicates that correlations
587 of AD with age were mainly observed in conjunction with FA and RD, and not with FA alone. This
588 would not be surprising given that most studies to date show greater RD changes than AD, and
589 oThis pattern was previously reported by Burzynska and colleagues (2010), who also showed
590 some areas of overlap with MD within this pattern. Interestingly, another study did not report
591 this pattern, but instead only observed AD changes in conjunction with FA and RD, further
592 suggesting it is not a common pattern associated with the aging brain [33].

593

594 **The FA, RD and MD pattern**

595

596 The pattern of FA, RD and MD has been suggested to reflect chronic white matter fiber
597 degeneration [20]. This pattern has been observed in While earlier studies have reported
598 differences in all of three of these measures with aging, few have assessed their specific regional
599 overlap [20, 31, 64]. Findings from our study indicated that chronic WM degeneration was
600 observed in the CC, mainly in the regions of the body and genu as well as the body of the fornix.
601 Diffusion imaging studies have consistently reported white matter structural changes in the CC
602 with aging, particularly in the genu and body [20, 31, 33, 34, 62]. The CC is important for
603 interhemispheric communication, therefore chronic white matter impairments in this white
604 matter bundle could result in deficits in cognitive functions requiring cross communication

605 between hemispheres [68]. For example, many functional MRI studies have shown bilateral
606 activation in older adults compared to unilateral activation observed in younger adults, which
607 has been suggested to be a compensatory mechanism for declining networks and additional brain
608 recruitment for task performance [69-73]. It is plausible that this bilateral functional activation
609 often reported within frontal lobes in older adults may result from white matter alterations in
610 the CC affecting inter-hemispheric communication.

611

612 The fornix has previously been reported to show age-related structural changes [20, 31,
613 61, 74]. In contrast to our findings, a previous study found an overlap between FA, RD and MD
614 along with increases in AD in the body of the fornix [20], and another study that only assessed
615 FA, RD and AD, also found and overlap between all three measures in the fornix. It is important
616 to note that the fornix is located close to the ventricles, so measures within this structure may
617 be influenced by cerebrospinal fluid pulsation [74].

618

619 Although we found this pattern in some other white matter brain regions, again it was
620 not the main pattern, suggesting that chronic white matter degeneration is not linearly changing
621 across the brain with healthy aging.

622

623 **White matter hyperintensity load**

624

625 A recent study by Svärd and Colleagues (2017) showed that WMH load can impact FA and
626 MD measures in healthy elderly adults, and when comparing to prodromal Alzheimer's disease,

627 suggesting it may be essential to control for in any study assessing age effects on diffusion
628 measures of white matter [54]. Given that WMH load increases are observed with aging, it is
629 possible that some white matter differences between young and older healthy adults may be
630 attributable to disparate WMH load [75, 76]. Therefore, it may be important to measure WMH
631 load when assessing healthy aging, as well as neurodegenerative diseases to better understand
632 white matter changes that are specific to “normal appearing white matter”, and not driven by
633 white matter hyperintensities [54]. We performed the analysis in the same cohort without
634 including WMH load as a covariate (i.e. only NART and gender covariates were included in
635 correlation analysis) and found that adjusting for WMH load did not affect the results greatly in
636 this study. For this analysis one extra subject was included ($n = 80$; mean age = 43.65 ± 18.36 SD),
637 and the percentage of voxels correlated with age were minimally affected for each diffusion
638 measure: FA (positive = 0%; negative = 50.17%), RD (positive = 39.01%; negative = 0%), MD
639 (positive = 6.11%; negative = 0%) and AD (positive = 0.03%; negative = 31.63%) (see S1 Table).
640 The main difference was that no negative correlations of age with MD were observed. The
641 patterns of overlap, and percentages were also largely maintained (see S2 Table). It is worth
642 noting that with the exception of one subject, all WMH loads were in the lower range for all
643 subjects suggesting that our older adults were indeed healthy, and that perhaps subtler effects
644 would be expected in the current cohort. Nevertheless, few studies have taken WMH load into
645 account when assessing aging, and to our knowledge, none have assessed its effect on
646 percentages of voxels linearly associated with age or patterns of overlap between diffusion
647 measures. It is possible that discrepancies within aging studies may be accounted for, or at least
648 partially explained by white matter hyperintensity load effects on DTI measures. Future studies

649 of aging, or age-related diseases are needed to confirm the extent to which WMH load effects
650 DTI measures in various tracts throughout the brain.

651

652 **DTI data acquisition insights**

653

654 In the literature to date many TBSS studies of aging have used b-values of less than 1500,
655 and the two main studies we compared to by Burzynska and colleagues (2010), and Bennett and
656 colleagues (2010) both used b-values of 1000, whereas this study utilized diffusion weighted data
657 with a b-value of 2000. Increasing the b-value can be advantageous; for example, it increases the
658 brightness of white matter which may be beneficial to segmentation of gray and white matter
659 [77]. An increase in b-value from 1000 to 3000 has also been shown to result in noisier images,
660 loss of signal, and hyperintense white matter compared to gray matter [78]. The findings from
661 this study of statistically significant negative linear correlations of age with FA are consistent with
662 the literature, as well as the linear correlations with RD and AD. However, some dissimilar
663 findings were found, mainly with MD. It has been shown that increases in the b-value results in
664 decreases in the apparent diffusion coefficient but not FA measures, and changes in the diffusion
665 properties of gray and white matter [77, 79]. Discrepancies between studies may indeed be
666 explained by differences in data acquisition parameters. Further research focusing on differences
667 in scan acquisition and analysis techniques is needed to test this specifically. Overall, this study
668 found that a b-value of 2000 is still sensitive to detection of age-related changes in diffusion
669 measures of white matter in the brain, using a widely used analysis method. We also found very
670 similar patterns of overlap between FA, RD and AD diffusion parameters, observed in previous

671 studies. Any discrepancies may be in part due to differences in acquisition parameters and/or
672 various processing and analysis techniques.

673

674 **Limitations**

675

676 DTI-based measures of axonal integrity and myelination should be interpreted with
677 caution as these are indirect measures of white matter structural integrity. The TBSS technique
678 also has limitations. It is known that 90% of the brain white matter consists of crossing fibers,
679 however the diffusion tensor has difficulty in accounting for these crossing fibers [80]. Therefore,
680 DTI measures may not be true representations of fiber integrity in regions of crossing fibers.
681 Anatomical specificity inaccuracies of the TBSS analysis approach have also been reported, as
682 well as image registration [81]. Despite these limitations, this analysis has been utilized by many
683 studies. Importantly DTI studies of aging have reproduced results of post-mortem studies of the
684 brain proving it to be a useful technique.

685

686 **Conclusion**

687

688 This study quantified patterns of age-related linear correlations with diffusion measures
689 of white matter in a cohort of young, middle-aged and older adults. Overall this study found that
690 healthy aging has a profound impact on white matter. The patterns of age-related linear
691 correlations with diffusion measures provides crucial information about possible underlying

692 causes of degeneration of white matter, and how the various patterns of decline may be region
693 specific. These findings may have important implications for connectivity between brain regions
694 and the cognitive functions they support in healthy aging. The study emphasizes the importance
695 of considering patterns of white matter changes in DTI measures across adulthood, while
696 controlling for variables that may affect assessment of changes white matter with healthy aging.
697 This may help to better understand specific biological profile contributing to white matter
698 deterioration which may influence brain function in healthy aging.

699 **Acknowledgments**

700

701 The authors would like to thank the participants who donated their time and energy to
702 our research. The authors would also like to thank Sojo Josephs and the Trinity Centre for High
703 Performance Computing (TCHPC) for their support throughout the project.

705 References

706

707 1. Basser PJ, Pajevic S, Pierpaoli C, Duda J, Aldroubi A. In vivo fiber tractography using DT-MRI data.
708 Magnetic resonance in medicine. 2000;44(4):625-32.

709 2. Basser PJ, Pierpaoli C. Microstructural and physiological features of tissues elucidated by
710 quantitative-diffusion-tensor MRI. J Magn Reson B. 1996;111(3):209-19.

711 3. Pierpaoli C, Jezzard P, Basser PJ, Barnett A, Di Chiro G. Diffusion tensor MR imaging of the
712 human brain. Radiology. 1996;201(3):637-48.

713 4. Cavedo E, Lista S, Rojkova K, Chiesa PA, Houot M, Brueggen K, et al. Disrupted white matter
714 structural networks in healthy older adult APOE ϵ 4 carriers – An international multicenter DTI study.
715 Neuroscience. 2017;357:119-33.

716 5. Fischer FU, Scheurich A, Wegrzyn M, Schermuly I, Bokde ALW, Klöppel S, et al. Automated
717 tractography of the cingulate bundle in Alzheimer's disease: A multicenter DTI study. Journal of
718 Magnetic Resonance Imaging. 2012;36(1):84-91.

719 6. Cherubini A, Peran P, Spoletini I, Di Paola M, Di Iulio F, Hagberg GE, et al. Combined volumetry
720 and DTI in subcortical structures of mild cognitive impairment and Alzheimer's disease patients. Journal
721 of Alzheimer's disease : JAD. 2010;19(4):1273-82.

722 7. Inglesi M, Bester M. Diffusion imaging in multiple sclerosis: research and clinical implications.
723 NMR in biomedicine. 2010;23(7):865-72.

724 8. Keil C, Prell T, Peschel T, Hartung V, Dengler R, Grosskreutz J. Longitudinal diffusion tensor
725 imaging in amyotrophic lateral sclerosis. BMC neuroscience. 2012;13:141-.

726 9. O'Dwyer L, Lamberton F, Bokde ALW, Ewers M, Faluyi YO, Tanner C, et al. Multiple Indices of
727 Diffusion Identifies White Matter Damage in Mild Cognitive Impairment and Alzheimer's Disease. PLOS
728 ONE. 2011;6(6):e21745.

729 10. Alexander AL, Hurley SA, Samsonov AA, Adluru N, Hosseinbor AP, Mossahebi P, et al.
730 Characterization of cerebral white matter properties using quantitative magnetic resonance imaging
731 stains. *Brain Connect.* 2011;1(6):423-46.

732 11. Assaf Y, Pasternak O. Diffusion tensor imaging (DTI)-based white matter mapping in brain
733 research: a review. *Journal of molecular neuroscience : MN.* 2008;34(1):51-61.

734 12. Schmierer K, Scaravilli F, Altmann DR, Barker GJ, Miller DH. Magnetization transfer ratio and
735 myelin in postmortem multiple sclerosis brain. *Annals of neurology.* 2004;56(3):407-15.

736 13. Song SK, Sun SW, Ju WK, Lin SJ, Cross AH, Neufeld AH. Diffusion tensor imaging detects and
737 differentiates axon and myelin degeneration in mouse optic nerve after retinal ischemia. *NeuroImage.*
738 2003;20(3):1714-22.

739 14. Song SK, Sun SW, Ramsbottom MJ, Chang C, Russell J, Cross AH. Dysmyelination revealed
740 through MRI as increased radial (but unchanged axial) diffusion of water. *NeuroImage.* 2002;17(3):1429-
741 36.

742 15. Budde MD, Kim JH, Liang HF, Schmidt RE, Russell JH, Cross AH, et al. Toward accurate diagnosis
743 of white matter pathology using diffusion tensor imaging. *Magnetic resonance in medicine.*
744 2007;57(4):688-95.

745 16. Glenn OA, Henry RG, Berman JI, Chang PC, Miller SP, Vigneron DB, et al. DTI-based three-
746 dimensional tractography detects differences in the pyramidal tracts of infants and children with
747 congenital hemiparesis. *Journal of magnetic resonance imaging : JMRI.* 2003;18(6):641-8.

748 17. Sun SW, Liang HF, Le TQ, Armstrong RC, Cross AH, Song SK. Differential sensitivity of in vivo and
749 ex vivo diffusion tensor imaging to evolving optic nerve injury in mice with retinal ischemia.
750 *NeuroImage.* 2006;32(3):1195-204.

751 18. Ashtari M, Cervellione KL, Hasan KM, Wu J, McIlree C, Kester H, et al. White matter
752 development during late adolescence in healthy males: a cross-sectional diffusion tensor imaging study.
753 *NeuroImage*. 2007;35(2):501-10.

754 19. Sidaros A, Engberg AW, Sidaros K, Liptrot MG, Herning M, Petersen P, et al. Diffusion tensor
755 imaging during recovery from severe traumatic brain injury and relation to clinical outcome: a
756 longitudinal study. *Brain*. 2008;131(Pt 2):559-72.

757 20. Burzynska AZ, Preuschhof C, Backman L, Nyberg L, Li SC, Lindenberger U, et al. Age-related
758 differences in white matter microstructure: region-specific patterns of diffusivity. *NeuroImage*.
759 2010;49(3):2104-12.

760 21. Bennett IJ, Madden DJ. Disconnected aging: cerebral white matter integrity and age-related
761 differences in cognition. *Neuroscience*. 2014;276:187-205.

762 22. Malloy P, Correia S, Stebbins G, Laidlaw DH. Neuroimaging of white matter in aging and
763 dementia. *The Clinical neuropsychologist*. 2007;21(1):73-109.

764 23. Barrick TR, Charlton RA, Clark CA, Markus HS. White matter structural decline in normal ageing:
765 a prospective longitudinal study using tract-based spatial statistics. *NeuroImage*. 2010;51(2):565-77.

766 24. Madden DJ, Bennett IJ, Burzynska A, Potter GG, Chen NK, Song AW. Diffusion tensor imaging of
767 cerebral white matter integrity in cognitive aging. *Biochim Biophys Acta*. 2012;1822(3):386-400.

768 25. Madden DJ, Bennett IJ, Song AW. Cerebral white matter integrity and cognitive aging:
769 contributions from diffusion tensor imaging. *Neuropsychol Rev*. 2009;19(4):415-35.

770 26. Tang Y, Nyengaard JR, Pakkenberg B, Gundersen HJ. Age-induced white matter changes in the
771 human brain: a stereological investigation. *Neurobiology of aging*. 1997;18(6):609-15.

772 27. Meier-Ruge W, Ulrich J, Brühlmann M, Meier E. Age-related white matter atrophy in the human
773 brain. *Ann N Y Acad Sci*. 1992;673:260-9.

774 28. Sullivan EV, Pfefferbaum A. Neuroradiological characterization of normal adult ageing. *Br J*
775 *Radiol.* 2007;80 Spec No 2:S99-108.

776 29. Nusbaum AO, Tang CY, Buchsbaum MS, Wei TC, Atlas SW. Regional and global changes in
777 cerebral diffusion with normal aging. *AJNR Am J Neuroradiol.* 2001;22(1):136-42.

778 30. O'Sullivan M, Jones DK, Summers PE, Morris RG, Williams SC, Markus HS. Evidence for cortical
779 "disconnection" as a mechanism of age-related cognitive decline. *Neurology.* 2001;57(4):632-8.

780 31. Zahr NM, Rohlfing T, Pfefferbaum A, Sullivan EV. Problem solving, working memory, and motor
781 correlates of association and commissural fiber bundles in normal aging: a quantitative fiber tracking
782 study. *NeuroImage.* 2009;44(3):1050-62.

783 32. Cox SR, Ritchie SJ, Tucker-Drob EM, Liewald DC, Hagenaars SP, Davies G, et al. Ageing and brain
784 white matter structure in 3,513 UK Biobank participants. *Nat Commun.* 2016;7:13629.

785 33. Bennett IJ, Madden DJ, Vaidya CJ, Howard DV, Howard JH, Jr. Age-related differences in multiple
786 measures of white matter integrity: A diffusion tensor imaging study of healthy aging. *Hum Brain Mapp.*
787 2010;31(3):378-90.

788 34. Davis SW, Dennis NA, Buchler NG, White LE, Madden DJ, Cabeza R. Assessing the effects of age
789 on long white matter tracts using diffusion tensor tractography. *NeuroImage.* 2009;46(2):530-41.

790 35. Madden DJ, Spaniol J, Costello MC, Bucur B, White LE, Cabeza R, et al. Cerebral white matter
791 integrity mediates adult age differences in cognitive performance. *J Cogn Neurosci.* 2009;21(2):289-302.

792 36. Zhong WJ, Guo DJ, Zhao JN, Xie WB, Chen WJ, Wu W. Changes of axial and radial diffusivities in
793 cerebral white matter led by normal aging. *Diagn Interv Imaging.* 2012;93(1):47-52.

794 37. de Groot M, Cremers LG, Ikram MA, Hofman A, Krestin GP, van der Lugt A, et al. White Matter
795 Degeneration with Aging: Longitudinal Diffusion MR Imaging Analysis. *Radiology.* 2016;279(2):532-41.

796 38. Lebel C, Gee M, Camicioli R, Wieler M, Martin W, Beaulieu C. Diffusion tensor imaging of white
797 matter tract evolution over the lifespan. *NeuroImage.* 2012;60(1):340-52.

798 39. Sullivan EV, Pfefferbaum A. Diffusion tensor imaging and aging. *Neurosci Biobehav Rev.*
799 2006;30(6):749-61.

800 40. Salat DH, Tuch DS, Hevelone ND, Fischl B, Corkin S, Rosas HD, et al. Age-related changes in
801 prefrontal white matter measured by diffusion tensor imaging. *Ann N Y Acad Sci.* 2005;1064:37-49.

802 41. Sullivan EV, Rohlfing T, Pfefferbaum A. Longitudinal study of callosal microstructure in the
803 normal adult aging brain using quantitative DTI fiber tracking. *Dev Neuropsychol.* 2010;35(3):233-56.

804 42. Westlye LT, Walhovd KB, Dale AM, Bjørnerud A, Due-Tonnessen P, Engvig A, et al. Life-span
805 changes of the human brain white matter: diffusion tensor imaging (DTI) and volumetry. *Cereb Cortex.*
806 2010;20(9):2055-68.

807 43. Zhang Y, Du AT, Hayasaka S, Jahng GH, Hlavin J, Zhan W, et al. Patterns of age-related water
808 diffusion changes in human brain by concordance and discordance analysis. *Neurobiology of aging.*
809 2010;31(11):1991-2001.

810 44. Buckner RL, Head D, Parker J, Fotenos AF, Marcus D, Morris JC, et al. A unified approach for
811 morphometric and functional data analysis in young, old, and demented adults using automated atlas-
812 based head size normalization: reliability and validation against manual measurement of total
813 intracranial volume. *NeuroImage.* 2004;23(2):724-38.

814 45. Schmidt P, Gaser C, Arsic M, Buck D, Forschler A, Berthele A, et al. An automated tool for
815 detection of FLAIR-hyperintense white-matter lesions in Multiple Sclerosis. *NeuroImage.*
816 2012;59(4):3774-83.

817 46. Irfanoglu MO, Walker L, Sarlls J, Marenco S, Pierpaoli C. Effects of image distortions originating
818 from susceptibility variations and concomitant fields on diffusion MRI tractography results. *NeuroImage.*
819 2012;61(1):275-88.

820 47. Leemans A, Jones DK. The B-matrix must be rotated when correcting for subject motion in DTI
821 data. *Magnetic resonance in medicine.* 2009;61(6):1336-49.

822 48. Tax CM, Otte WM, Viergever MA, Dijkhuizen RM, Leemans A. REKINDLE: robust extraction of
823 kurtosis INDices with linear estimation. *Magnetic resonance in medicine*. 2015;73(2):794-808.

824 49. Smith SM, Jenkinson M, Woolrich MW, Beckmann CF, Behrens TE, Johansen-Berg H, et al.
825 Advances in functional and structural MR image analysis and implementation as FSL. *NeuroImage*.
826 2004;23 Suppl 1:S208-19.

827 50. Smith SM, Jenkinson M, Johansen-Berg H, Rueckert D, Nichols TE, Mackay CE, et al. Tract-based
828 spatial statistics: voxelwise analysis of multi-subject diffusion data. *NeuroImage*. 2006;31(4):1487-505.

829 51. Winkler AM, Ridgway GR, Webster MA, Smith SM, Nichols TE. Permutation inference for the
830 general linear model. *NeuroImage*. 2014;92:381-97.

831 52. Bright P, Jaldow E, Kopelman MD. The National Adult Reading Test as a measure of premorbid
832 intelligence: a comparison with estimates derived from demographic variables. *Journal of the*
833 *International Neuropsychological Society : JINS*. 2002;8(6):847-54.

834 53. Dunst B, Benedek M, Koschutnig K, Jauk E, Neubauer AC. Sex differences in the IQ-white matter
835 microstructure relationship: a DTI study. *Brain and cognition*. 2014;91:71-8.

836 54. Svard D, Nilsson M, Lampinen B, Latt J, Sundgren PC, Stomrud E, et al. The effect of white matter
837 hyperintensities on statistical analysis of diffusion tensor imaging in cognitively healthy elderly and
838 prodromal Alzheimer's disease. *PLoS One*. 2017;12(9):e0185239.

839 55. Smith SM, Nichols TE. Threshold-free cluster enhancement: addressing problems of smoothing,
840 threshold dependence and localisation in cluster inference. *NeuroImage*. 2009;44(1):83-98.

841 56. Kennedy KM, Raz N. Aging white matter and cognition: differential effects of regional variations
842 in diffusion properties on memory, executive functions, and speed. *Neuropsychologia*. 2009;47(3):916-
843 27.

844 57. Sibilia F, Kehoe EG, Farrell D, Kerskens C, O'Neill D, McNulty JP, et al. Aging-Related
845 Microstructural Alterations Along the Length of the Cingulum Bundle. *Brain Connect*. 2017;7(6):366-72.

846 58. Sun SW, Liang HF, Trinkaus K, Cross AH, Armstrong RC, Song SK. Noninvasive detection of
847 cuprizone induced axonal damage and demyelination in the mouse corpus callosum. Magnetic
848 resonance in medicine. 2006;55(2):302-8.

849 59. Kraus MF, Susmaras T, Caughlin BP, Walker CJ, Sweeney JA, Little DM. White matter integrity
850 and cognition in chronic traumatic brain injury: a diffusion tensor imaging study. Brain. 2007;130(Pt
851 10):2508-19.

852 60. Counsell SJ, Shen Y, Boardman JP, Larkman DJ, Kapellou O, Ward P, et al. Axial and radial
853 diffusivity in preterm infants who have diffuse white matter changes on magnetic resonance imaging at
854 term-equivalent age. Pediatrics. 2006;117(2):376-86.

855 61. Sullivan EV, Rohlfing T, Pfefferbaum A. Quantitative fiber tracking of lateral and
856 interhemispheric white matter systems in normal aging: relations to timed performance. Neurobiology
857 of aging. 2010;31(3):464-81.

858 62. Rojkova K, Volle E, Urbanski M, Humbert F, Dell'Acqua F, Thiebaut de Schotten M. Atlasing the
859 frontal lobe connections and their variability due to age and education: a spherical deconvolution
860 tractography study. Brain structure & function. 2015.

861 63. Wahl M, Li YO, Ng J, Lahue SC, Cooper SR, Sherr EH, et al. Microstructural correlations of white
862 matter tracts in the human brain. NeuroImage. 2010;51(2):531-41.

863 64. Mella N, de Ribaupierre S, Eagleson R, de Ribaupierre A. Cognitive intraindividual variability and
864 white matter integrity in aging. ScientificWorldJournal. 2013;2013:350623.

865 65. Schmahmann JD, Pandya DN, Wang R, Dai G, D'Arceuil HE, de Crespigny AJ, et al. Association
866 fibre pathways of the brain: parallel observations from diffusion spectrum imaging and autoradiography.
867 Brain. 2007;130(Pt 3):630-53.

868 66. Lawes IN, Barrick TR, Murugam V, Spierings N, Evans DR, Song M, et al. Atlas-based
869 segmentation of white matter tracts of the human brain using diffusion tensor tractography and
870 comparison with classical dissection. *NeuroImage*. 2008;39(1):62-79.

871 67. Wakana S, Jiang H, Nagae-Poetscher LM, van Zijl PC, Mori S. Fiber tract-based atlas of human
872 white matter anatomy. *Radiology*. 2004;230(1):77-87.

873 68. Reuter-Lorenz PA, Stanczak L. Differential effects of aging on the functions of the corpus
874 callosum. *Dev Neuropsychol*. 2000;18(1):113-37.

875 69. Reuter-Lorenz PA, Jonides J, Smith EE, Hartley A, Miller A, Marshuetz C, et al. Age differences in
876 the frontal lateralization of verbal and spatial working memory revealed by PET. *J Cogn Neurosci*.
877 2000;12(1):174-87.

878 70. Reuter-Lorenz PA, Lustig C. Brain aging: reorganizing discoveries about the aging mind. *Current
879 opinion in neurobiology*. 2005;15(2):245-51.

880 71. Cabeza R. Hemispheric asymmetry reduction in older adults: the HAROLD model. *Psychology
881 and aging*. 2002;17(1):85-100.

882 72. Cabeza R, Anderson ND, Locantore JK, McIntosh AR. Aging gracefully: compensatory brain
883 activity in high-performing older adults. *NeuroImage*. 2002;17(3):1394-402.

884 73. Park DC, Reuter-Lorenz P. The adaptive brain: aging and neurocognitive scaffolding. *Annual
885 review of psychology*. 2009;60:173-96.

886 74. Gunbey HP, Ercan K, Findikoglu AS, Bulut HT, Karaoglanoglu M, Arslan H. The limbic degradation
887 of aging brain: a quantitative analysis with diffusion tensor imaging. *ScientificWorldJournal*.
888 2014;2014:196513.

889 75. Raz N, Yang Y, Dahle CL, Land S. Volume of white matter hyperintensities in healthy adults:
890 contribution of age, vascular risk factors, and inflammation-related genetic variants. *Biochim Biophys
891 Acta*. 2012;1822(3):361-9.

892 76. Yoshita M, Fletcher E, Harvey D, Ortega M, Martinez O, Mungas DM, et al. Extent and
893 distribution of white matter hyperintensities in normal aging, MCI, and AD. *Neurology*.
894 2006;67(12):2192-8.

895 77. Yoshiura T, Wu O, Zaheer A, Reese TG, Sorensen AG. Highly diffusion-sensitized MRI of brain:
896 dissociation of gray and white matter. *Magnetic resonance in medicine*. 2001;45(5):734-40.

897 78. Burdette JH, Durden DD, Elster AD, Yen YF. High b-value diffusion-weighted MRI of normal brain.
898 *Journal of computer assisted tomography*. 2001;25(4):515-9.

899 79. DeLano MC, Cooper TG, Siebert JE, Potchen MJ, Kuppusamy K. High-b-value diffusion-weighted
900 MR imaging of adult brain: image contrast and apparent diffusion coefficient map features. *AJNR Am J
901 Neuroradiol*. 2000;21(10):1830-6.

902 80. Jeurissen B, Leemans A, Tournier JD, Jones DK, Sijbers J. Investigating the prevalence of complex
903 fiber configurations in white matter tissue with diffusion magnetic resonance imaging. *Hum Brain Mapp*.
904 2013;34(11):2747-66.

905 81. Bach M, Laun FB, Leemans A, Tax CM, Biessels GJ, Stieltjes B, et al. Methodological
906 considerations on tract-based spatial statistics (TBSS). *NeuroImage*. 2014;100:358-69.

907

908 **Supporting Information**

909

910 **S1Table. Total number and percentage of voxels correlated with age, and the overlap of MD,**

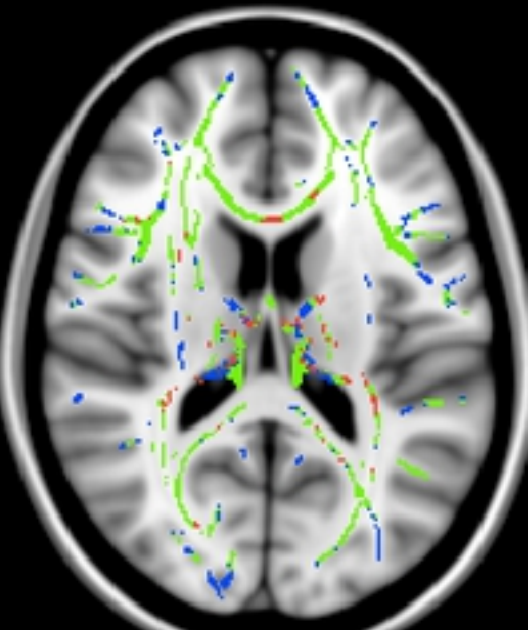
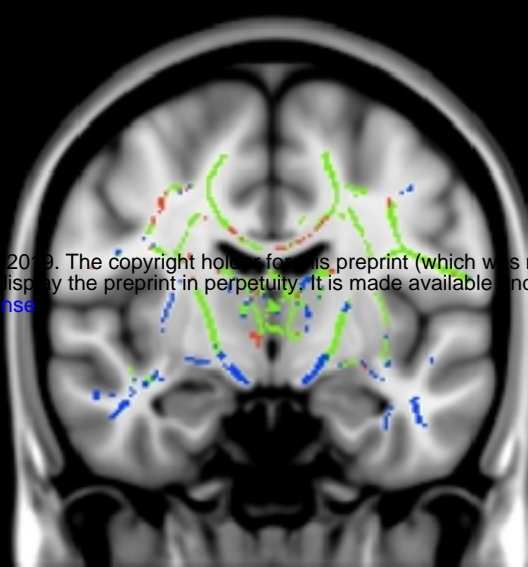
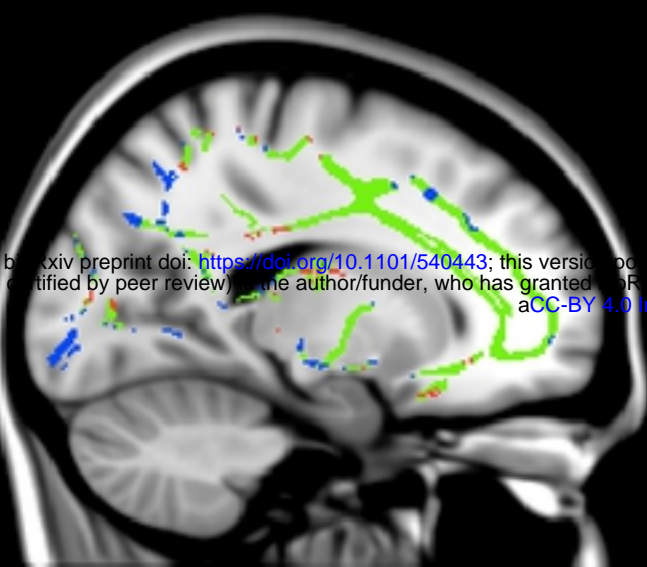
911 **RD and AD with age-related FA voxels.** NART and gender were included as covariates.

912

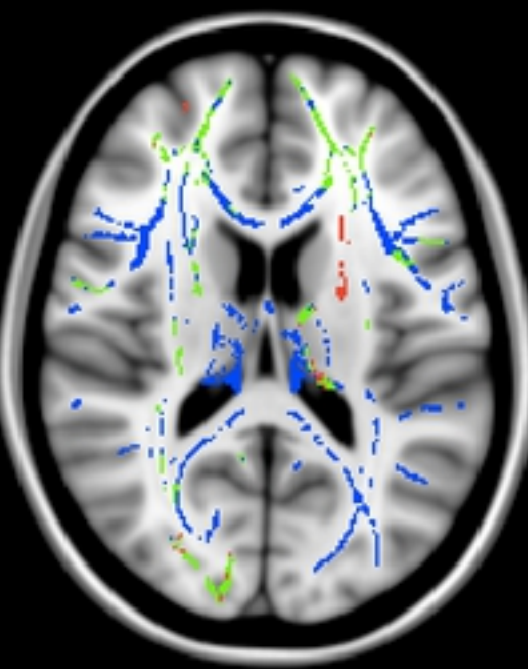
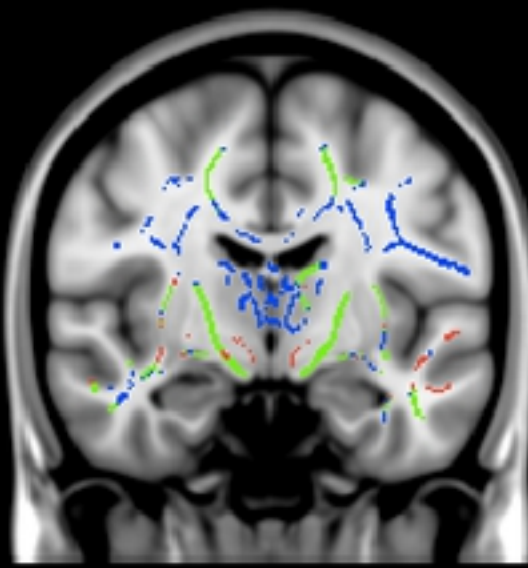
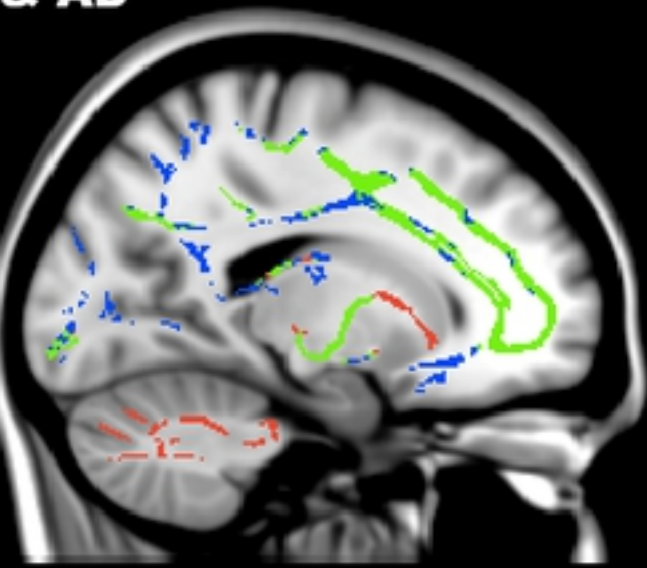
913 **S2 Table. Total number and percentage of voxels correlated with age showing specific patterns**

914 **of overlap between diffusion measure.** NART and gender were included as covariates.

FA & RD



FA & AD



FA & MD

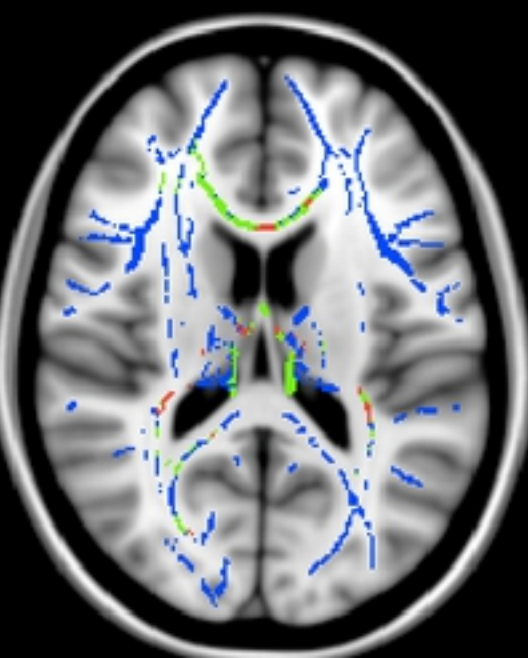
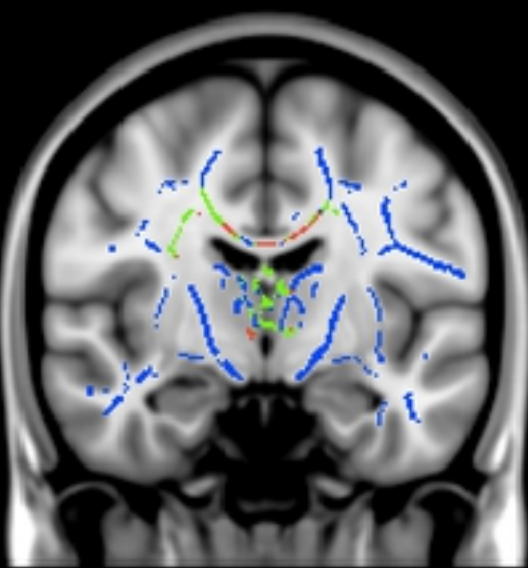
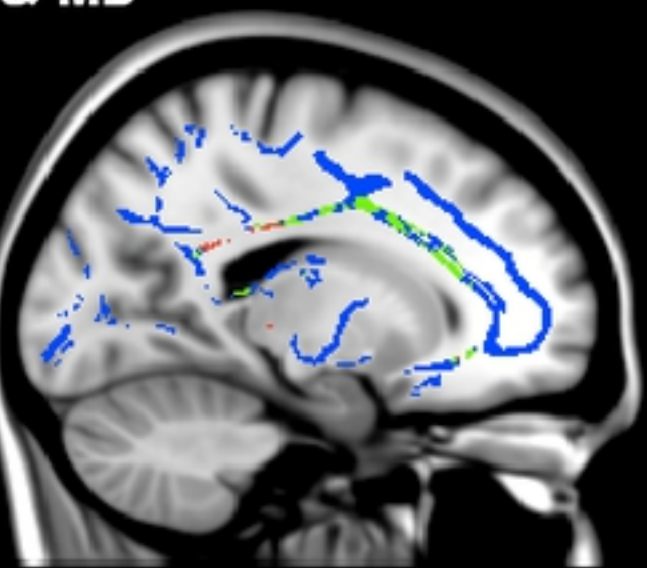
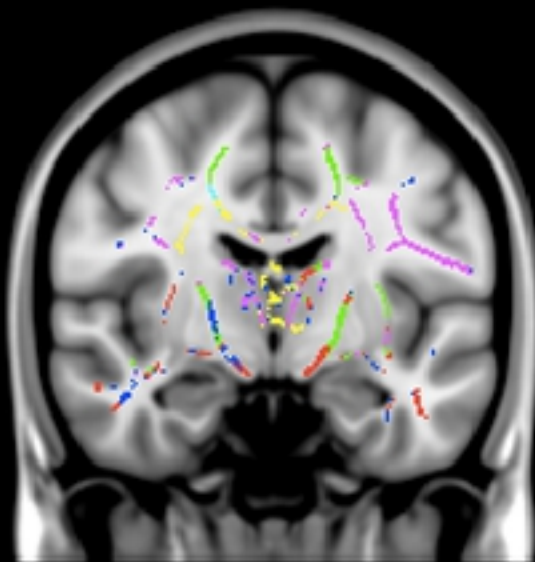
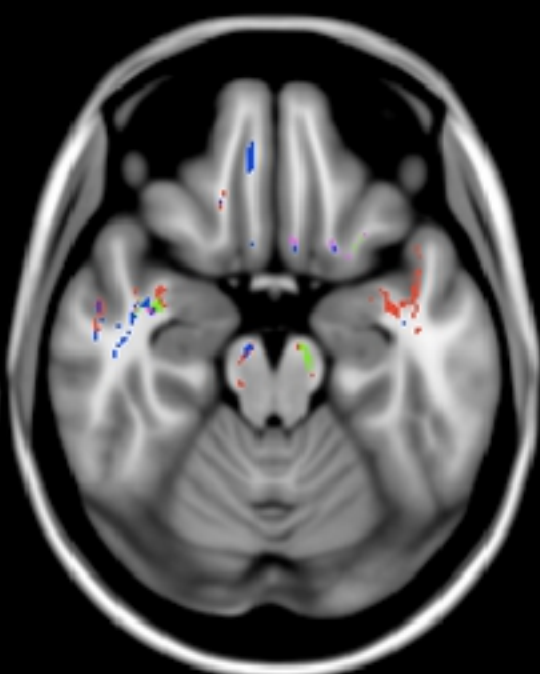


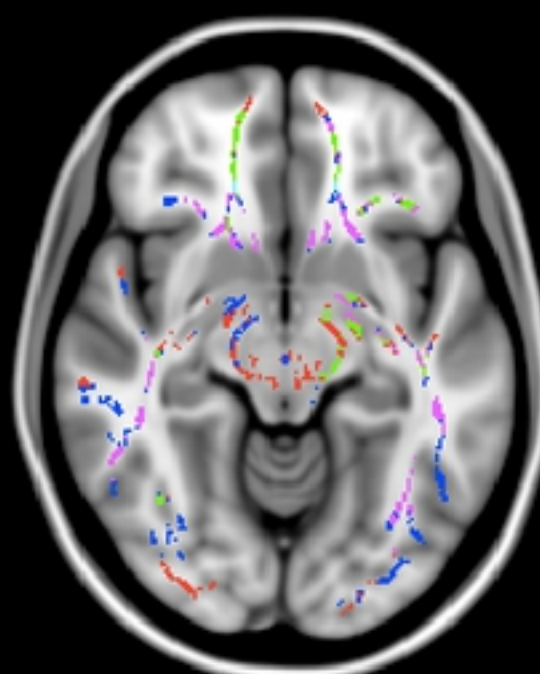
Figure 1



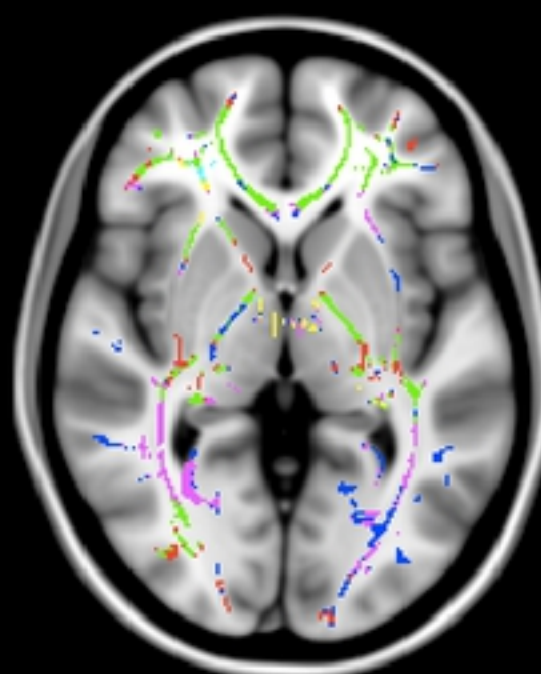
$y = -10$



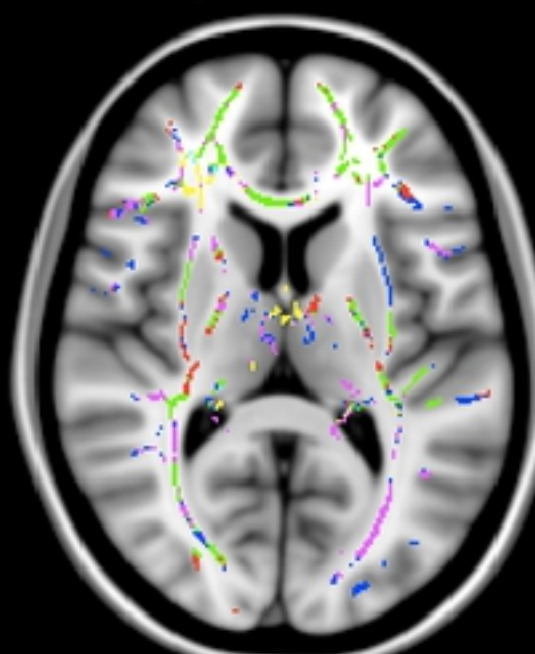
$z = -20$



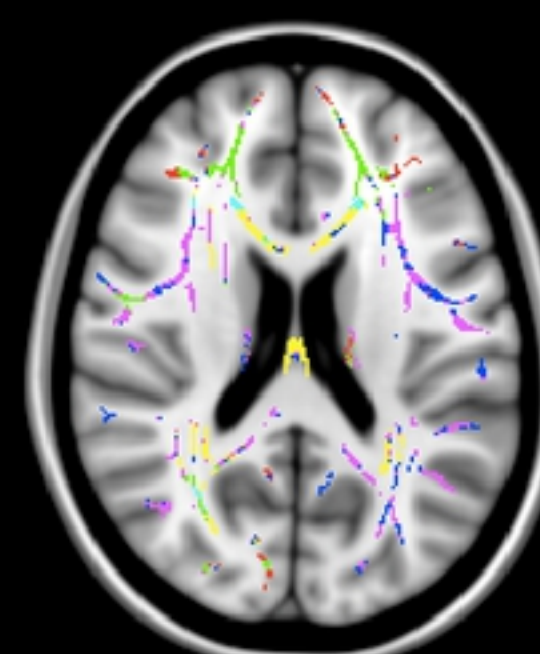
$z = -10$



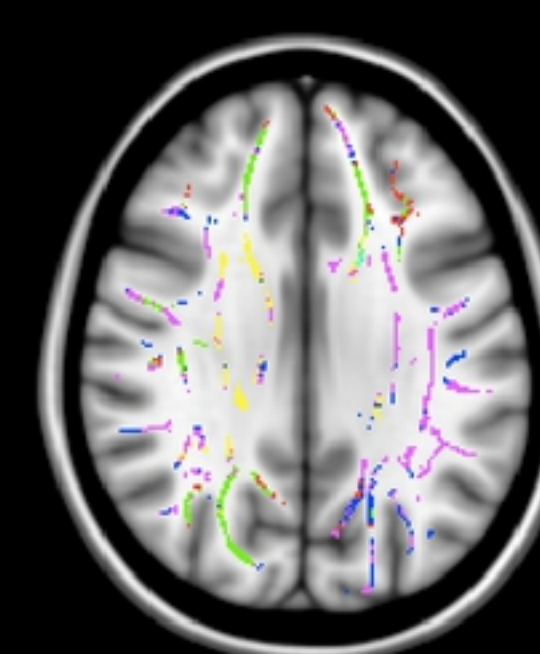
$z = 0$



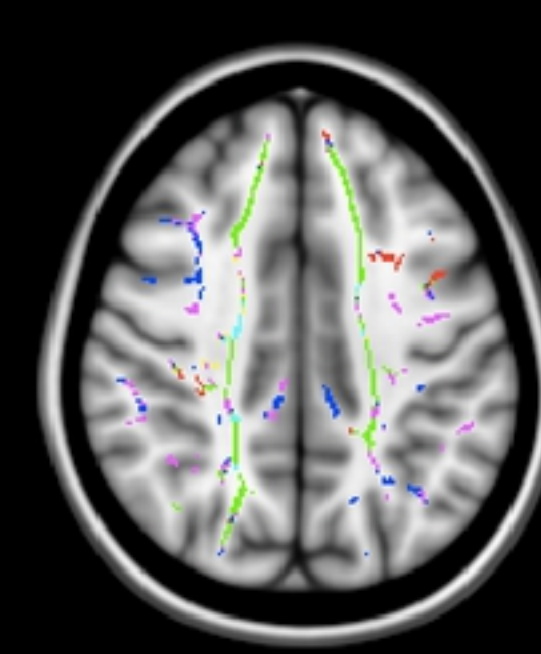
$z = 10$



$z = 20$



$z = 30$



$z = 40$

Figure2